A Summary of "A new tri-particle backlighter for high-energy-density plasmas"

Rishabh Datta
(Dated: December 9, 2021)

Background. Proton radiography (or proton imaging [1]) is a technique used to measure the time- and spatially-resolved magnetic and electric fields in High-Energy-Density (HED) plasmas[1][2][3][4]. A proton source backlighter generates beams of energetic particles, which are deflected by the electric and magnetic fields within the plasma of interest. From the particle deflection, we reconstruct the fields which caused the deflection. Compared to other commonly used magnetic diagnostics, such as Faraday rotation (which measures the line-integrated product of electron density and the magnetic field $\int n_e \mathbf{B}\cdot\mathbf{dl}$), and inductive probes (which provide spatially localized measurements, and are limited by their size and plasma environment), proton radiography has the advantage of measuring both the magnitude and direction of the path-integrated magnetic field in the object plane.

In proton radiography, the charged particle source is typically either the ICF implosion of D^3He fuel-filled capsules [1][3], or the laser-driven acceleration of protons from thin foils (called TNSA) [5][6]. There are some key differences between both methods. First, the ICF particles have discrete energies, while TNSA particles exhibit a continuous spectrum. Monoenergetic particles minimize the ambiguity and degeneracy associated with the measurement of deflection of polyenergetic particles [2][1]. Secondly, TNSA generates a directed flow of protons with a smaller angular spread, while the ICF capsule generates an isotropic particle flux; this reduces asymmetries in the deflection due to spatial gradients in the particle flux [2]. Finally, TNSA provides excellent spatial resolution comparable to the size of the focal spot ($\sim 5-10\,\mu m$). For the ICF capsule, the spatial resolution, which depends on the size of the hotspot, is larger ($\sim 40-50\,\mu m$ FWHM) [2].

Figure 1A shows a typical proton imaging setup. We relate the position $\mathbf{r_0}$ and intensity I_0 in the object plane (which contains a plasma of length a) to that in the image plane using [2]:

$$\mathbf{r} = \frac{l}{L}\mathbf{r_0} + L\boldsymbol{\alpha} \tag{1}$$

$$I \approx I_0(1 - \nabla_0 \cdot \boldsymbol{\alpha}) \tag{2}$$

Where l is the source-plasma distance, L is the plasma-detector distance, and $\boldsymbol{\alpha}$ is the deflection vector. To derive Eq. (1), we assume (i) a point source and uniform particle fluence, (ii) the paraxial limit, i.e. $l \gg a$, (iii) the charged species do not alter the dynamics of the plasma, and (iv) high magnification limit, i.e. $L \gg l$ [2]. Furthermore, to get Eq. (2), we assume a low contrast parameter $\mu \equiv l|\alpha|/a \ll 1$. A large contrast parameter can introduce singularities (called caustics) in the detector intensity [2], which make it difficult to uniquely reconstruct the electric and magnetic fields, so it is advantageous to operate in the low μ regime [2]. The contrast parameter depends not only on l/L (which we control experimentally), but also on the deflection $|\boldsymbol{\alpha}|$, which varies with field strength and particle energy, so it is important to pick experimental parameters (experimental geometry and particle energy) that ensure that $|\boldsymbol{\alpha}| \ll a/l$ is satisfied to avoid caustics.

From (1) & (2), we can reconstruct the position of the fields which cause the deflection $\boldsymbol{\alpha}$. The deflection due to the electric $\mathbf{E}$ and magnetic fields $\mathbf{B}$ within the plasma are [2]:

$$\begin{aligned} \boldsymbol{\alpha}_B &= \frac{q}{\sqrt{2mW}} \int \mathbf{dl} \times \mathbf{B} \\ \boldsymbol{\alpha}_E &= \frac{q}{2W} \int \mathbf{E}\, dl \end{aligned} \tag{3}$$

Here, q, m, and W are the particle charge, mass, and kinetic energy respectively. The magnitude of deflection scales as $\sim W^{-1/2}$ for the magnetic field, and $\sim W^{-1}$ for the electric field. By comparing the deflection of species with different energies, we can uniquely isolate the contributions of the two fields. In addition to field deflection, particles also undergo collisional deflection, which scales as $\alpha_s \propto q^2 n_e L/W$. Collisional scattering can become significant, especially for low-energy particles, in high-density plasmas such as in ICF Holhraums.

Diagnostic Summary. This paper [1] uses the laser-driven ICF implosion of a DT^3He filled capsule to generate three quasi-monoenergetic particles - (i) 14.7 MeV D^3He protons, (ii) 3 MeV DD protons, and (iii) 9.5 MeV T^3He deuterons, for proton imaging of a laser-driven plasma bubble. The authors fill a $860\,\mu m$ glass capsule with 120 atm DT^3He, with the atomic ratio chosen to maximize T^3He reaction yield. 59 OMEGA laser beams (pulse duration ~0.6 ns, energy $\sim$ 29 kJ) irradiate the capsule to drive the ICF implosion of the fuel, which undergoes the

[1] Although called an imaging technique, there is no 1-1 mapping of the object and the image due to field-induced deflections

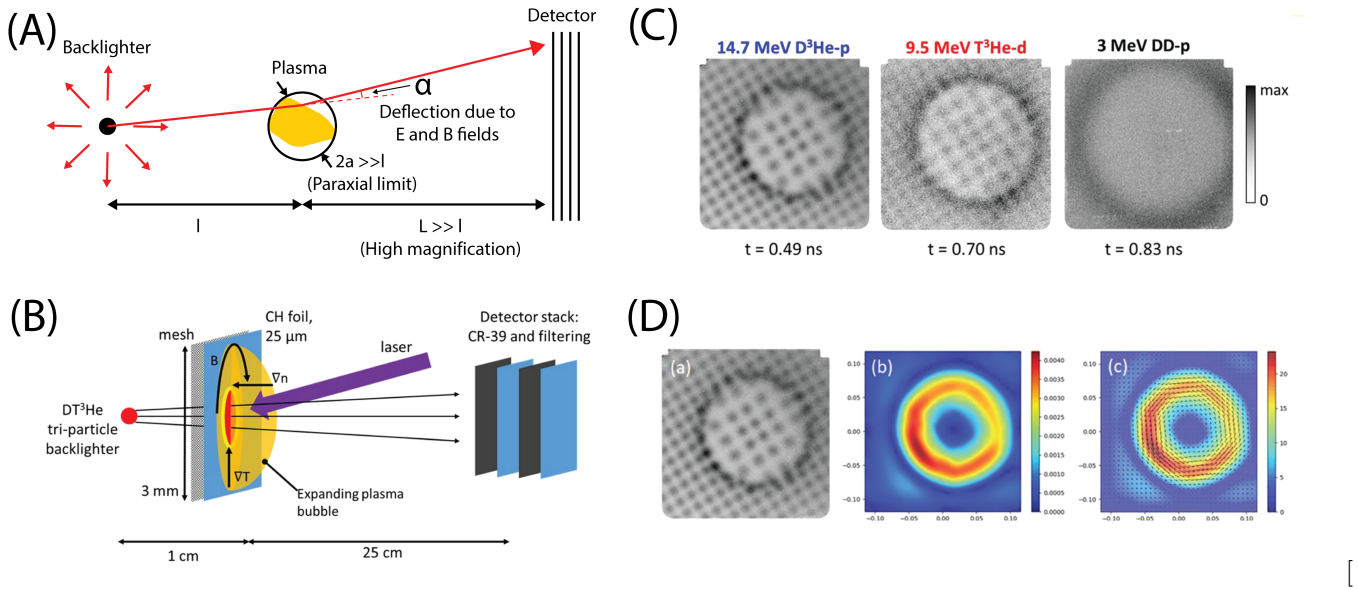

FIG. 1. (A) Schematic of a typical proton imaging diagnostic setup. (B) Experimental and diagnostic setup. Proton imaging with a DT^{3}He backlighter is used to determine the azimuthal magnetic field produced by non-parallel electron density and temperature gradients in the plasma bubble. (C) Radiographs measured by the CR-39 detector stack. The fastest-moving 14.7 MeV protons arrive first, and the slowest moving 3 MeV protons arrive last. The 3 MeV protons are heavily scattered due to collisions. (D) Deflection map and reconstructed transverse path-integrated magnetic field determined from the D^{3}He proton radiograph. Adapted from: Sutcliffe, et al. RSI 92, (2021).

following reactions:

$$\begin{aligned} \mathrm{D} + \mathrm{D} &\rightarrow \mathrm{T} + p\,(3.0\,\mathrm{MeV}) \\ \mathrm{D} + {}^3\mathrm{He} &\rightarrow {}^4\mathrm{He} + p\,(14.7\,\mathrm{MeV}) \\ \mathrm{T} + {}^3\mathrm{He} &\rightarrow {}^4\mathrm{He} + d\,(9.5\,\mathrm{MeV}) \end{aligned} \tag{4}$$

A laser beam impinges on the backside of a plastic (CH) foil to generate a plasma bubble (Figure 1B). The Biermann battery effect ($\partial_t B \propto \nabla T \times \nabla n_e$) generates azimuthal magnetic fields, which cause radial deflection of the charged particles. Although the authors do not provide characteristic plasma parameters in this experiment, similar plasma bubble experiments typically exhibit density, temperature, and magnetic fields of $n_e \sim 10^{20}\,\mathrm{cm}^{-3}$, $T_{e,i} \sim 0.5\,\mathrm{keV}$, and $B \sim 0.5\,\mathrm{MG}$ respectively [7].

A mesh collimates the particle beams into an array of beamlets (a technique called 'grid deflectometry' [4]), which then travel through the plasma bubble, and are detected by a stack of CR-39 detectors. The charged particles leave trails of molecular damage in the CR-39. Particles with different energy have different trail characteristics, which are used to distinguish the particles [2].

Since particles with different energies exhibit different times-of-flight to the plasma, they also probe the plasma at different times. The fast-moving 14.7 MeV protons provide information at early time (t = 0.49 ns), while the slower moving 9.5 MeV deuterons provide information at a later time (t = 0.7 ns) (Figure 1C). The lowest energy 3 MeV DD protons are scattered away in this experiment, so they do not provide useful radiography data. From the deflection of the beamlet structure, the authors reconstruct the transverse path-integrated magnetic field, as shown in Figure 1D. The field is azimuthal in direction and the magnitude is $\overline{BL} \sim$ 10-20 MG-μm.

Discussion. The DT^{3}He backlighter, with three monoenergetic charged species, is a direct improvement over the D^{3}He backlighter, which only generates two charged species — 3 MeV DD protons and 14.7 MeV D^{3}He protons. The additional T^{3}He 9.5 MeV deuterons provide several key advantages:

(1) **Time-resolved data**: While the D^{3}He backlighter provides information at a maximum of two distinct times (and therefore only provides information of the first time-derivative of measured quantities), the DT^{3}He backlighter diagnoses the plasma at 3 distinct times (separated by $\sim 100\,\mathrm{ps}$), and provides the second time-derivative of measured quantities.

(2) **High-density and high-field probing**: Collisional scattering scales as $\propto n^2/W$, and field deflection increases with field strength and decreases with increasing W, so in high-density high-field environ-

[2] 3 MeV protons and 9.5 MeV deuterons are collected on the first CR-39 plate. 14.7 MeV protons are collected on the second CR-39 plate after passing through an Aluminum filter.

ments, where the lowest energy 3 MeV protons are lost, the higher-energy 9.5 MeV deuterons can still probe the plasma.

(3) **Field distinction**: Differences in scaling of magnetic and electric deflection with W allow us to isolate the contribution of the two fields. The T^3He 9.5 MeV deuterons provide additional data for comparison of deflections in the same experimental shot, reducing the uncertainty in reconstruction. This is especially useful in high-density environments where the lower energy 3 MeV protons would be scattered away.

The authors do not provide uncertainty bounds for the calculated magnetic field. Uncertainty in the spatial structure of the field depends on the diagnostic's spatial resolution, which is limited by gaussian broadening due to a finite source size, non-uniformity of the backlighter flux, and broadening at the plasma and detector [2] [3]. Furthermore, using grid deflectometry to create beamlets sacrifices spatial resolution for clarity.

The temporal uncertainty of the measurement is set by the fusion burn time ($\sim$ 150 ps), and the Doppler broadening of the particle energies. The authors show that the Doppler broadening of the particle energies (due to thermal distribution of the fusion reactants) is small $\sim$ 100 keV, and leads to a temporal uncertainty of only $\sim$ 20 ps in this experiment, which is small compared to the burn duration.

The spatial resolution can be improved by increasing the backlighter yield. The fusion particle yield over duration τ and volume V scales as:

$$Y_{ij} = n_i n_j \langle \sigma v \rangle_{ij} \tau V \tag{5}$$

Here, n is the density, σ is the reaction cross-section, and v is the velocity. Higher fusion yields can be achieved by increasing the fusion volume or the burn duration. However, as discussed by the authors, this cannot be done without sacrificing spatial and temporal resolution.

The DT^3He backlighter suffers from many of the same limitations of the D^3He backlighter. The number of diagnosable times within an experimental shot is restricted to a maximum of three. One way to overcome this limitation is to use multiple backlighters placed at different locations (hence, different times-of-flight), or imploded at different times. Furthermore, if we use the 3.5 MeV α-particles generated by the DT reaction, and the 4.8 MeV α-particles from the T^3He reaction, we can access additional probing times, and get more information about the electric and magnetic fields. These ideas have been introduced in [3], but the authors do not discuss them here.

Other limitations of this method are harder to overcome. The highest particle energy achievable with the DT^3He is 14.7 MeV (compared to $\sim$ 60 MeV for TNSA [5]). Collisional scattering means that the D^3He backlighter cannot be used for very dense plasmas (where the 17 MeV protons are scattered away). Furthermore, the ICF implosion in this experiment was driven by a subset of the OMEGA laser beams, which limits the laser power available to drive the actual plasma experiment. The reproducibility of the ICF implosion also limits effective comparison between experimental shots using the same backlighter, or between different backlighters within the same shot. Reproducibility of the proton and deuteron yields depends on several factors, including capsule size and fill, gas atomic ratio, and laser power. The contrast parameter must also be low to prevent caustics. For very strong fields, the lower-energy particles are prone to caustic generation because of large deflection angles.

Summary. The authors present a tri-particle radiography diagnostic with a DT^3He backlighter for studying HED plasmas. The DT^3He backlighter is a direct improvement over the D^3He backlighter. The authors diagnose the plasma at an addition time instance, probe higher-density and higher-field plasmas, and better distinguish between electric and magnetic contributions to the deflection. The diagnostic is demonstrated on a laser-driven plasma bubble, where it is used to determine the path-integrated transverse magnetic field. Although the uncertainty in the measured field is not discussed, the DT^3He backlighter provides excellent temporal resolution ($\sim$ 100 ps), and spatial resolution can be adjusted by varying the yield and size of the fusion volume to fit the experimental goals.

[1] G. Sutcliffe *et al.*, Review of Scientific Instruments **92**, 10.1063/5.0043845 (2021).

[2] N. L. Kugland *et al.*, Review of Scientific Instruments **83**, 10.1063/1.4750234 (2012).

[3] C. K. Li *et al.*, Review of Scientific Instruments **77**, 10.1063/1.2228252 (2006).

[4] A. J. Mackinnon *et al.*, Review of Scientific Instruments **75**, 10.1063/1.1788893 (2004).

[5] S. C. Wilks *et al.*, Physics of Plasmas **8**, 10.1063/1.1333697 (2001).

[6] R. A. Snavely *et al.*, Physical Review Letters **85**, 10.1103/PhysRevLett.85.2945 (2000).

[7] M. J. Rosenberg *et al.*, Physical Review E - Statistical, Nonlinear, and Soft Matter Physics **86**, 10.1103/PhysRevE.86.056407 (2012).